

# Analysis and characterization of longitudinal flux single-sided linear switched reluctance machines

Lenin CHOKKALINGAM<sup>1,\*</sup>, Rengasamy ARUMUGAM<sup>2</sup>

<sup>1</sup>*Department of Electrical Engineering, St. Joseph's College of Engineering,  
Chennai-INDIA*

<sup>2</sup>*Department of Electrical Engineering, SSN College of Engineering,  
Chennai-INDIA*

*e-mail: nclenin@gmail.com*

Received: 19.05.2010

## Abstract

*Linear switched reluctance motors (LSRMs) have recently gained more popularity for propulsion drives. This paper contributes a certain design improvement to reduce the force ripple in LSRMs. By affixing a pole cap in the stator pole, the target is achieved. Finite element analysis has been carried out to predict the performance of the basic and proposed structures. Motor performances for different load conditions are simulated. The application of fast Fourier transform has been utilized to envisage the vibration frequencies. The experimental results are well correlated with the predicted results.*

**Key Words:** *Linear switched reluctance motor, pole cap, ripple, FFT*

## 1. Introduction

The absence of permanent magnets, the presence of windings in either the stator or translator (moving part), and a high fault tolerance are some of the notable features of linear switched reluctance motors (LSRMs) [1]. In the recent past, many design concepts, control techniques, and converter structures have been studied to improve the performance of the LSRM [2-8]. Recently in [9], sensitivity analysis of double-sided LSRM parameters was presented.

In this paper, a stator structure for a longitudinal flux LSRM is implemented to reduce the force ripple. Two-dimensional (2D) finite element analysis (FEA) is extensively utilized to envisage the performance of the basic and proposed structures.

If the frequency of the stimulating force is close or identical to any of the natural frequencies, then resonance occurs in electrical machines [10]. The fast Fourier transform (FFT) is used to predict the ripple in the force profile. The sway of load difference on some parameters like velocity, current, and the efficiency of the motor are studied.

---

\*Corresponding author: Department of Electrical Engineering, St. Joseph's College of Engineering, Chennai-INDIA

The organization of this paper is as follows: Section 2 predicts the performance of the 2 stator structures by means of FEA; for various load conditions, the machine performance is simulated in Section 3; to determine the resonance frequencies, FFT is used in Section 4; experimental results are presented in Section 5; and conclusions and upcoming studies are summarized in Section 6.

## 2. LSRM stator with pole cap

The 2D cross-sectional view of the basic LSRM is shown in Figure 1. The entire machine specifications are tabulated in Table 1. In this basic structure, the stator pole is rectangular in nature.

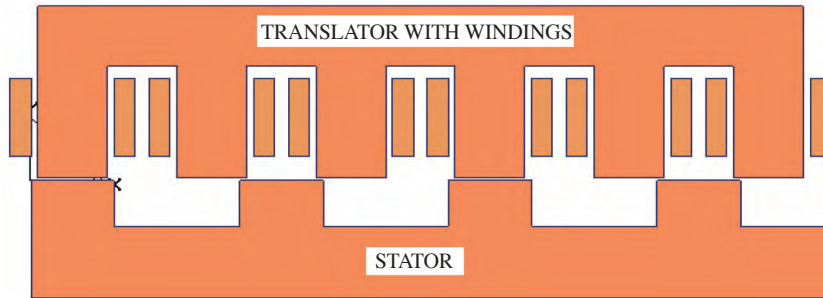


**Figure 1.** 2D cross-sectional view of the conventional LSRM.

**Table 1.** Specifications and dimensions of the basic LSRM.

$l_g = 1.5 \text{ mm}$	$w_{sp} = 21 \text{ mm}$
$F_{\max} = 120 \text{ N}$	$h_{sp} = 30 \text{ mm}$
$L_{stack} = 40 \text{ mm}$	$w_{sy} = 35 \text{ mm}$
Steel type (stator) = M 45	$w_{ss} = 31 \text{ mm}$
Steel type (translator) = M 45	$w_{ts} = 26 \text{ mm}$
Travel length = 2 m	$h_{tp} = 48 \text{ mm}$
$V_{rated} = 120 \text{ V}$	$w_{tp} = 13 \text{ mm}$
$I_{rated} = 10 \text{ A}$	$w_{ty} = 30 \text{ mm}$
$N_{ph} = 396$	Wire size = AWG 18

Electromagnetic field analysis was carried out with the rated current of 10 A. The predicted propulsion force and inductance profiles for various stator pole widths are shown in Figure 2. Table 2 summarizes the comparison of the studied configuration.

The aim of this study is to improve the performance of the LSRM by suppressing the force ripple. Pole caps are introduced on the poles of the stator. Figure 3 shows the difference between the 2 stator poles. The 2D view of the proposed LSRM is shown in Figure 4. Electromagnetic field analysis was repeated to predict the performance of the proposed structure for various stator pole widths. The predicted profiles are plotted in Figure 5. Table 4 gives the comparison of the FEA results for both of the structures.

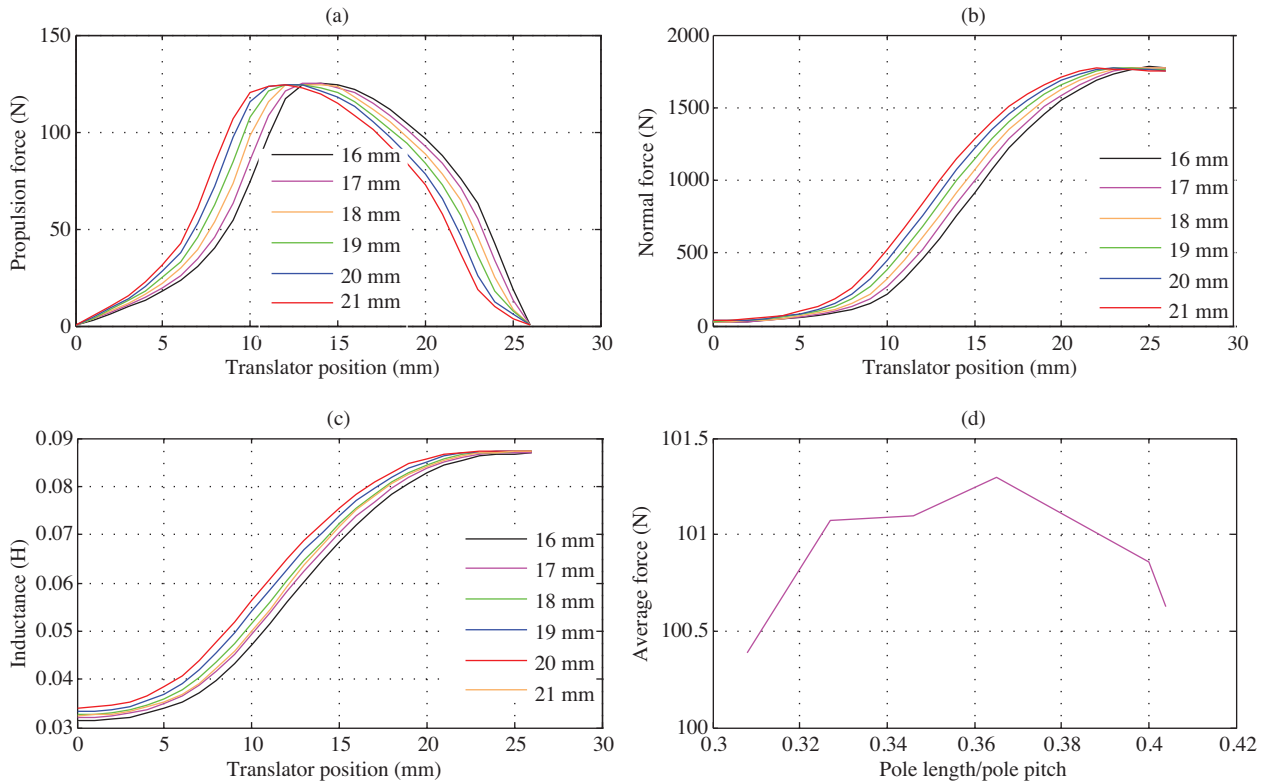


**Figure 2.** Force and inductance for various stator pole widths (without pole caps).

**Table 2.** Comparison of the force ripple for various stator pole widths (without pole caps).

$W_{sp}$ (mm)	Pole pitch Pole pitch	$F_{min}$ (N)	$F_{max}$ (N)	$F_{avg}$ (N)	% force ripple	$L_{min}$ L(H)	$L_{max}$ (H)
16	0.308	67.33	124.87	100.39	60.38	0.02972	0.08626
17	0.327	67.91	124.70	101.07	57.68	0.03019	0.08658
18	0.346	68.23	124.57	101.10	55.88	0.03071	0.08683
19	0.365	68.32	124.11	101.30	53.41	0.03125	0.087
20	0.4	68.28	124.34	100.86	56.16	0.03184	0.08713
21	0.404	67.88	123.90	100.63	55.67	0.03246	0.08725

**Table 3.** Comparison of the force ripple for various stator pole widths (with pole caps).

$W_{sp}$ (mm)	Pole pitch Pole pitch	$F_{min}$ (N)	$F_{max}$ (N)	$F_{avg}$ (N)	% force ripple	$L_{min}$ L(H)	$L_{max}$ (H)
16	0.357	69.30	123.33	100.2	53.97	0.03130	0.08681
17	0.368	68.83	122.76	100.74	53.54	0.03194	0.08708
18	0.379	68.84	122.18	100.72	52.95	0.03260	0.08723
19	0.389	68.62	121.78	100.98	52.64	0.03327	0.08730
20	0.4	68.27	121.77	100.70	53.12	0.03403	0.08737

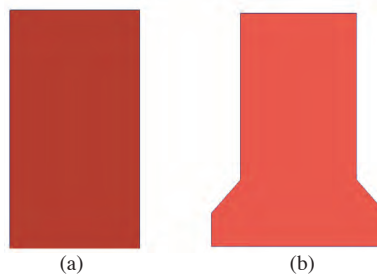


**Figure 3.** Difference between the stator poles: a) conventional, b) proposed.

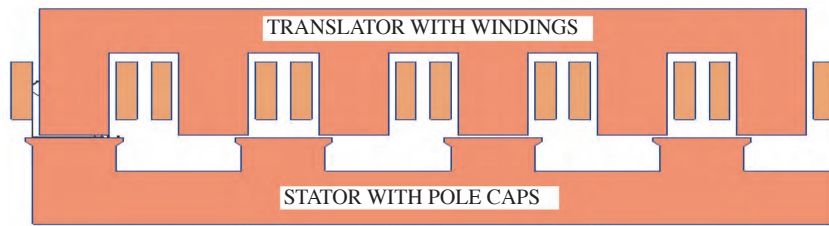


**Figure 4.** 2D cross-sectional view of the proposed LSRM.

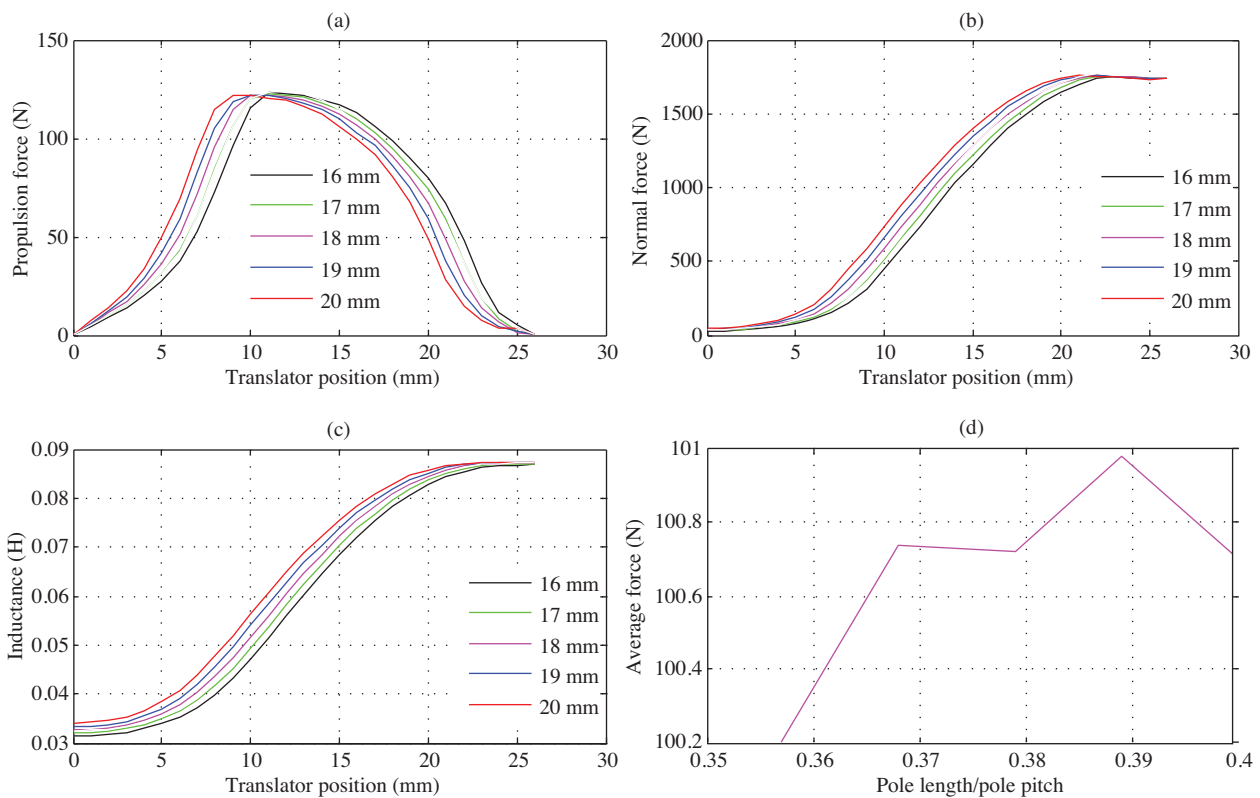


**Figure 5.** Force and inductance for various stator pole widths (with pole caps).

**Table 4.** Comparison of the volume, mass and force ripple.

$W_{sp}$ (mm)	Volume (m <sup>3</sup> )		Mass (kg)		% of force ripple		Force ripple reduction (%)
	Without caps	With caps	Without caps	With caps	Basic	Proposed	
16	0.00243	0.00238	18.68	18.37	60.38	53.97	10.62
17	0.00245	0.00242	18.88	18.64	57.68	53.54	7.18
18	0.00247	0.00245	19.1	18.92	55.88	52.95	5.24
19	0.0025	0.00249	19.28	19.19	53.41	52.64	1.44
20	0.00253	0.00252	19.48	19.46	56.16	53.12	5.41
21	0.00255	NA	19.67	NA	55.67	NA	NA

### 3. Prediction of motor performance for variable load circumstances

The cause of load variation on parameters like velocity, current, mechanical power, and the efficiency of the motor were studied. The results are tabulated in Table 5.

**Table 5.** Influence of the load on motor performance.

$F_L$ (N)	I (A)	V (m/s)	Input power (W)	Output power (W)	Efficiency (%)
2	2.09	10.42	57.85	26.12	45.15
5	3.28	8.03	65.84	31.46	47.78
10	4.72	6.40	91.39	39	42.67
20	5.31	4.02	114.61	46.99	41
40	6.19	3.35	151.36	57.70	38.12
60	7.87	2.65	181.32	63.66	35.11
80	8.29	1.28	196.36	67	34.12
100	9.79	0.5	214.45	71.11	33.16
120	10.5	0.15	255.84	77.8	30.41

Figure 6a shows the velocity and current profiles for various load conditions. The velocity decreases with an increase in the load. Figure 6b demonstrates the feature of mechanical power,  $P_m$ , and efficiency. It can be seen that initially, as the load increases, the efficiency increases, and when the load is further increased, the efficiency starts to decrease. Figure 6c illustrates the feature of the efficiency with an alteration in the mechanical power  $P_m$ .

### 4. Application of fast Fourier transform

It is first necessary to find the force versus the translator position from the 2D FEA. The FFT is then applied to the force profile. The available force versus the translator position profile was converted into the force versus time profile. Figure 7 shows the results of the FFT for the case of a stator with and without pole caps. The frequency corresponding to these dB peaks can be identified from the design. Table 6 provides the dominant frequencies in Hz and amplitudes in dB for both structures. It is observed that the dB peaks occur at certain similar frequencies (without pole caps), but the magnitude of the dB peaks is reduced in the proposed structure.

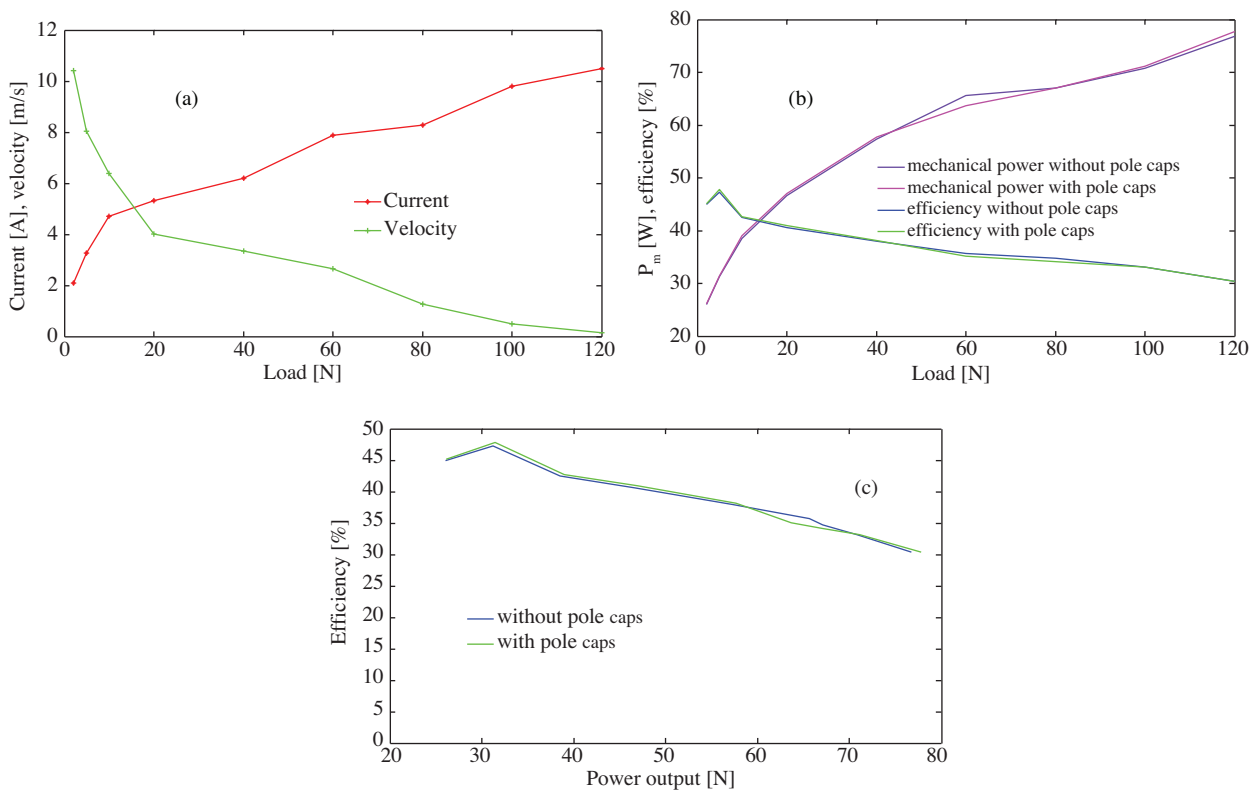


**Figure 6.** a) Variation of the current and velocity with a load; b) variation of  $P_m$  and efficiency with a load; c) variation of efficiency with  $P_m$ .

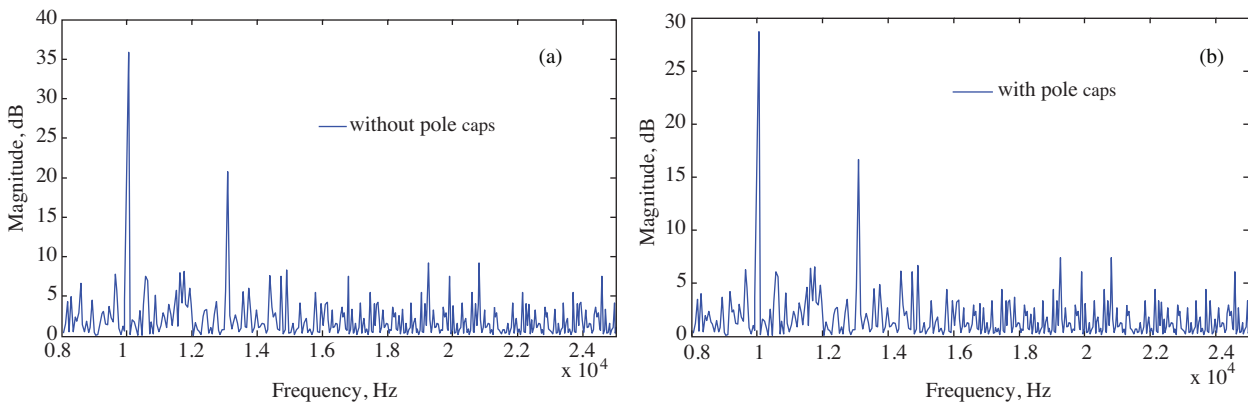


**Figure 7.** FFT output: a) without pole cap, b) with pole cap.

## 5. Experimental results

Figure 8 shows the experimental system for the LSRM with the stator pole cap. The stator is 2 m in length. The translator has a mass of 12 kg. Figure 9 shows the voltage, current, and inductance waveforms of the LSRM. The inductance values are closely correlated with the predicted values.

**Table 6.** Ripple frequencies and their amplitudes for the stator, with and without pole caps.

Predominant ripple frequencies (Hz)		Amplitude (dB)	
Stator without pole caps	Stator with pole caps	Stator without pole caps	Stator with pole caps
10,050	10,050	35.85	28.68
13,100	14,620	20.8	16.64
14,910	19,260	8.29	7.348
19,260	22,420	9.185	7.21

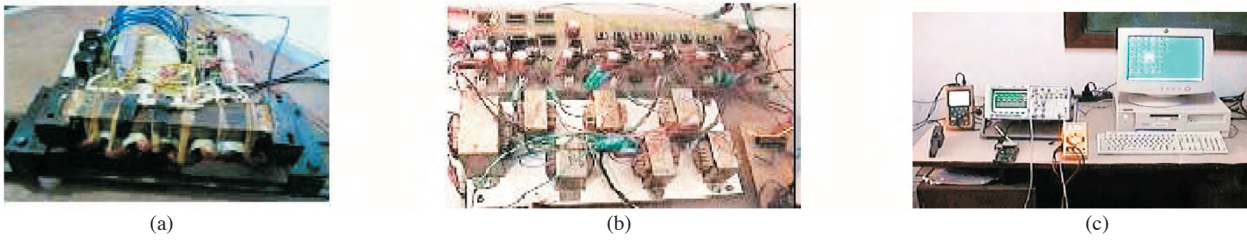


**Figure 8.** Experimental setup of: a) the LSRM and converter, b) the driver circuit, c) the PC along with measuring instruments.

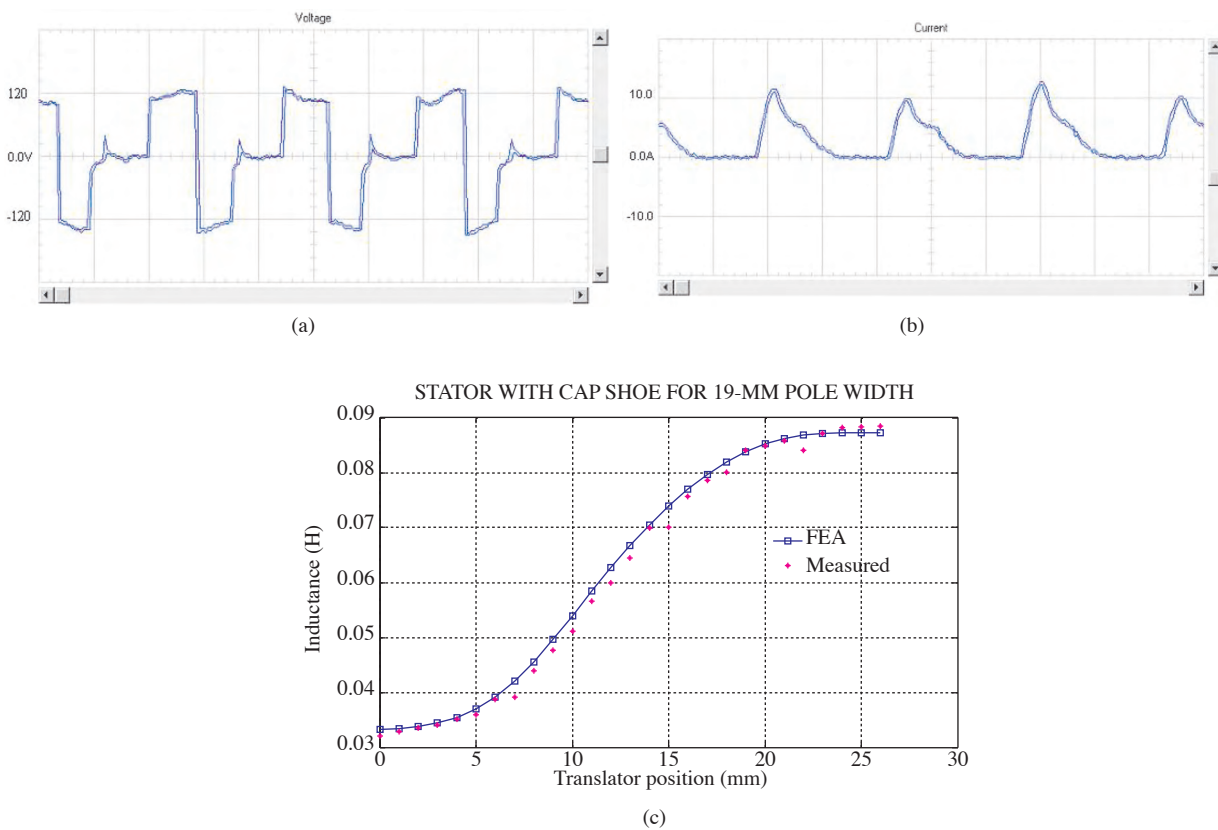


**Figure 9.** Experimental waveforms during single pulse operation: a) actual phase voltage of the LSRM, b) actual phase current of the LSRM, c) inductance profile.

## 6. Conclusion

A design variation to mitigate the force ripple by the provision of stator pole caps has been presented. A prototype LSRM was simulated and experimentally validated. The following conclusions were observed compared to the basic machine: a) the force ripple was decreased by 5%, b) the volume of the stator was decreased by 3%, c) the mass of the stator was reduced by 2.5%, and d) from the FFT analysis, the peak amplitude (dB) was 20% less.

## Nomenclature

$K_{sp}$	Width of the stator pole (m)	$l_g$	Air gap length (m)
$K_{ss}$	Width of the stator slot (m)	$V_{rated}$	Rated voltage (V)
$K_{sy}$	Stator back iron thickness (m)	$I_{rated}$	Rated current (A)
$h_{sp}$	Stator pole height (m)	$F_{max}$	Maximum force (N)
$K_{tp}$	Width of the translator pole (m)	$F_{min}$	Minimum force (N)
$K_{ts}$	Width of the translator slot (m)	$F_{avg}$	Average force (N)
$K_{ty}$	Translator back iron thickness (m)	$F_L$	Load force (N)
$h_{tp}$	Translator pole height (m)	$P_m$	Mechanical power output (W)
$K_{spt}$	Width stator pole tip (m)	$N_{ph}$	No. of turns per phase
$K_{spw}$	Width stator pole width (m)	$L_{stack}$	Stack length (m)
		$L_{min}$	Minimum inductance (H)
		$L_{max}$	Maximum inductance (H)

## References

- [1] T.J.E. Miller, *Switched Reluctance Motors and Their Control*, Hillsboro, Ohio, Magna Physics, 1993.
- [2] B.S. Lee, H.K. Bae, P. Vijayraghavan, R. Krishnan, "Design of a linear switched reluctance machine", *IEEE Transactions on Industry Applications*, Vol. 36, pp. 1571–1580, 2000.
- [3] N. Chayopitak, D.G. Taylor, "Design of linear variable reluctance motor using computer-aided design assistant", *IEEE International Conference on Electric Machines and Drives*, pp. 1569–1575, 2005.
- [4] Z. Sun, N.C. Cheung, J. Pan, S.W. Zhao, W.C. Gan, "Design and simulation of a magnetic levitated switched reluctance linear actuator system for high precision application", *IEEE International Symposium on Industrial Electronics*, pp. 624–629, 2008.
- [5] U.S. Deshpande, J.J. Cathey, E. Richter, "High-force density linear switched reluctance machine", *IEEE Transactions on Industry Applications*, Vol. 31, pp. 345–352, 1995.
- [6] J. Pan, N.C. Cheung, J. Yang, "High-precision position control of a novel planar switched reluctance motor", *IEEE Transactions on Industrial Electronics*, Vol. 52, pp. 1644–1652, 2005.
- [7] S.W. Zhao, N.C. Cheung, W.C. Gan, J.M. Yang, J.F. Pan, "A self-tuning regulator for the high-precision position control of a linear switched reluctance motor", *IEEE Transactions on Industrial Electronics*, Vol. 54, pp. 2425–2434, 2007.
- [8] L. Kolomeitsev, D. Kraynov, F. Pakhomin, F. Rednov, E. Kallenbach, V. Kireev, T. Schneider, J. Böcker, "Linear switched reluctance motor as high efficiency propulsion system for railway vehicles", *International Symposium on Power Electronics, Electrical Drives, Automation and Motion*, pp. 155–160, 2008.
- [9] J.G. Amoros, P. Andrada, "Sensitivity analysis of geometrical parameters on a double-sided linear switched reluctance motor", *IEEE Transactions on Industrial Electronics*, Vol. 57, pp. 311–319, 2010.
- [10] D.E. Cameron, J.H. Lang, S.D. Umans, "The origin and reduction of acoustic noise in doubly salient variable-reluctance motors", *IEEE Transactions on Industry Applications*, Vol. 28, pp. 1250–1255, 1992.